
Copper Catalysts Supported on CeMnO₂ for CO Oxidation in Hydrogen-Rich Gas Streams

N. Hoshyar, A. Irankhah*, M. Jafari

Hydrogen and Fuel Cell Research Laboratory, Chemical Engineering Department,
University of Kashan, Kashan, Iran

Abstract

The CeMnO₂ supports were prepared via co-precipitation method by ammonia as precipitating agent. The CuO/CeO₂ and CuO/Ce_(1-x)Mn_xO₂ (x=0.1, 0.3 and 0.5) catalysts were synthesized by wet impregnation method. The physicochemical properties of the prepared CuO/Ce_(1-x)Mn_xO₂ catalysts were characterized by N₂ adsorption-desorption, powder X-ray diffraction (XRD) and programmed H₂ temperature reduction (H₂-TPR). The effects of Cu and Mn loading were investigated on the catalytic performance. The findings illustrated that the 7% CuO/Ce_{0.9}Mn_{0.1}O₂ catalyst shows high activity for CO-PrOx. The high activity of 7% CuO/Ce_{0.9}Mn_{0.1}O₂ catalyst was ascribed to high surface area of the support, synergetic effects of CuO and CeO₂ and increases of the mobility of lattice oxygen in ceria by addition of MnO₂. The effects of presence of H₂O in the reaction feed stream, oxygen to CO ratio (λ) and gas hourly space velocity (GHSV) on the catalytic activity of 7% CuO/Ce_{0.9}Mn_{0.1}O₂ were evaluated. It was found that the best performance of 7% CuO/Ce_{0.9}Mn_{0.1}O₂ catalyst was obtained at $\lambda=2$, GHSV=20000 h⁻¹ and in addition, the presence of H₂O had negative effects on the activity of the catalyst. In the long term stability test, nearly 100% CO conversion was maintained for 50 h at 120°C with 70-80% CO₂ selectivity.

Keywords: Cu/CeMnO₂ Catalyst; CO oxidation; PrOx; Hydrogen

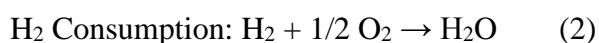
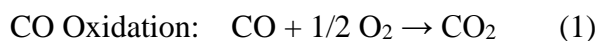
1. Introduction

Fuel cells are electrochemical devices, which directly convert fuels chemical energy into electrical energy with high efficiency and low environmental effects. Nowadays, fuel cells are among the main candidates in the development of clean and renewable energies [1]. Although there are various methods for hydrogen production, methane steam

reforming (MSR) is still the principal method for cost-effective hydrogen and synthesis gas production [2]. The preferential oxidation of CO (PrOx) is one of the critical steps in hydrogen production and purification for Polymer Electrolyte Fuel Cell (PEMFC); since the anode catalyst in PEM is strongly poisoned even by ppm levels of CO in the H₂ rich gas [3]. PrOx is used after steam reforming and WGS reactions to remove the trace contaminant CO in the H₂ rich gas.

* Corresponding author: irankhah@kashanu.ac.ir

Among the currently available methods, CO-PrOx is the most cost-effective and efficient approach to reduce CO to the desired level without excessive hydrogen consumption [4]. The main reactions involved in CO-PrOx are as follows:



Developed catalysts for CO-PrOx are mainly platinum group metals (Pt, Pd, Ru and Rh) catalysts [3-8,33], gold based catalysts [9-11] and transition metal (Co, Cu, and Mn) based catalysts [12-19,34]. Among them, CuO based on CeO₂ catalysts have shown high activity and selectivity for preferential oxidation of CO. Moreover, availability and low cost of ceria supported copper catalyst makes this catalyst a promising candidate to replace the other noble metals and gold. Copper and ceria based catalyst can be synthesized via different methods with a variety of morphologies by using various promoters and with different loading range of metals. Marino *et al.* synthesized the CuO-CeO₂ catalyst via homogeneous thermal decomposition of urea containing different Cu/Ce ratio [20]. CeCu10 catalyst kept constant nearly 90% CO conversion during 24 h of the reaction. Moretti *et al.* used a microcrystalline organized meso-porous γ -alumina prepared by template sol-gel method, resulting in, after impregnation with metal salts and subsequent calcination, active

Cu/Ce-based CO-PrOx catalysts with high surface area and a good thermal stability [21]. A Ce₂₀Cu₅ catalyst had complete CO conversion at 200°C with 40% CO₂ selectivity. Wu *et al.* prepared the CuO/CeO₂ by an improved incipient wetness impregnation method using ammonia as chelating agent [4]. The 10% CuO/CeO₂ had high activity and stability for CO-PrOx. In presence of 10% H₂O and 15% CO₂, 100% CO conversion and 75-85% CO₂ selectivity was reported. Pakharukova *et al.* tested the copper-cerium oxide catalysts supported on monoclinic zirconium oxide and showed that the best performance was obtained for the CuO/CeO₂/ZrO₂ catalysts containing 5-10 wt% copper [22]. Peng *et al.* synthesized the 7%CuO/Ce_{0.9}Mn_{0.1}O₂-20%Al₂O₃ catalyst with a T₁₀₀ temperature of 95–100°C [23]. This catalyst was evaluated for 200 h at 140°C in the presence of 15% CO₂ and 10% H₂O which exhibited 60% CO conversion and 95% CO₂ selectivity.

In the present study, the CeO₂ samples were prepared in different conditions of pH, calcination time and temperature and aging time and the optimum condition was achieved for CeO₂ as a support for Cu catalyst. Then the manganese, as a promoter, doped into CeO₂ to obtain the CeMn oxide as a new support for the above-mentioned catalyst. Moreover, Cu/Mn loading ratio was studied. In addition, Cu catalysts supported on CeO₂ and Ce_(1-x)Mn_xO₂ were prepared to investigate their catalytic activity in CO-PrOx reaction. Furthermore, more significant operating conditions such as GHSV, λ ratio

and presence of H₂O in feed composition were investigated to explore the best range of operating conditions for these catalysts.

2. Experimental

2-1. Catalyst preparation

0.1 M homogeneous aqueous solution of cerium nitrate was prepared by solving Ce(NO₃)₃.6H₂O [Fluka, 99.5%] powder in deionized water, then ammonia [NH₃, Merck, 25%] was added slowly to reach the desired pH (8-10). The resulting suspension was left to settle for 1-12 h. The precipitate was filtered and washed with deionized water several times. Finally, the ceria cake was dried overnight (in various temperature ranging from 80 to 120°C). The dried precipitate was calcined in different time and temperature (T_c=400-600°C and t_c=4-6 h). The Ceria which was synthesized in pH of 10, aged for 6 h, dried at 120°C and calcined in 500°C for 6 h had maximum surface area. The surface area of achieved ceria was 74.45 m²/g, with total pore volume of 0.18 m³/g and average pore diameter of about 9.6 nm.

CeMnO₂ samples were synthesized with co-precipitation of the manganese nitrate [Mn(NO₃)₂.4H₂O, Merck, 99.5%] and cerium nitrate in the optimum conditions of CeO₂, i.e. pH 10, aging time of 6 h, and calcinations temperature of 500°C for 6 h. Three different values (x=0.1, 0.3 and 0.5) of Mn were synthesized.

The CuO/Ce_(1-x)Mn_xO₂ catalysts were prepared by wetness impregnation method using different loadings (5, 7 and 10 wt%) of copper nitrate solution [Cu(NO₃)₂.3H₂O, Merck, 99.5%]. The catalysts were then dried at 120°C for 12 h and calcined at 500°C for 4 h in air.

2-2. Catalyst characterization

The XRD patterns were recorded on an X-ray diffractometer (PAN alytical X'Pert-Pro) using a Cu-K_α monochromatized radiation source and a Ni filter in the range 2θ=20- 80°.

The surface areas (BET), mean pore diameter and total pore volume were determined by nitrogen adsorption at -196°C, using an automated gas adsorption analyzer (Gimini, Micromeritics).

Temperature programmed reduction (TPR) analysis was used for evaluating the reduction properties of prepared catalysts. In the TPR measurement, the fresh catalyst (~100 mg) was exposed to a heat treatment (10°C/min up to 800°C) in a gas flow (30 ml/min) containing a mixture of 10 vol% H₂ in Argon. Before the TPR experiment, the samples were degassed under an inert atmosphere at 350°C for 3 h.

2-3. Catalytic activity tests

Catalytic activity tests were carried out at 60-200°C temperature range and ambient pressure in a fixed bed quartz reactor (8 mm inner diameter). In addition, 210 mg catalyst with 40-60 mesh was charged in the reactor for each test. Gas feed components are 2% CO, 2% O₂ and 96% H₂ with the space velocity of 20000 h⁻¹. Before the light-off tests, the catalysts were pretreated at 400°C for 1 h in O₂ stream with a flow rate of 20 ml/min. Inlet and outlet gases were analyzed by a Shimadzu-8A chromatograph equipped with a TCD and a Carbosieve column.

The CO and O₂ conversion were calculated based on the carbon monoxide and oxygen consumption in the reactions as follows:

$$X_{CO}(\%) = \frac{[CO_{in}] - [CO_{out}]}{[CO_{in}]} \times 100 \quad (1)$$

$$X_{O_2}(\%) = \frac{[O_{2in}] - [O_{2out}]}{[O_{2in}]} \times 100 \quad (2)$$

The CO₂ selectivity of CO oxidation reaction in presence of excess hydrogen was calculated from the oxygen mass balance as follows:

$$S_{CO_2}(\%) = 0.5 \times \left(\frac{[CO_{in}] - [CO_{out}]}{[O_{2in}] - [O_{2out}]} \right) \times 100 \quad (3)$$

The excess of oxygen factor (λ) is defined as:

$$\lambda = 2 \times \frac{F_{O_2}^{in}}{F_{CO}^{in}} \quad (4)$$

3. Results and discussion

3-1. Catalyst characterization

The XRD patterns of CeO₂, CuO/CeO₂ and CuO/CeMnO₂ catalysts are presented in Fig. 1. The crystalline mean particle sizes of ceria have been determined by the X-ray broadening technique employing the Scherrer equation as:

$$d_{XRD} = \frac{0.9 \lambda}{FWHM \cos \theta} \quad (5)$$

Where λ is the X-ray wavelength (1.5406 Å), FWHM (in Rad) is the full width at half maximum of the characteristic peak (111) of CeO₂ and θ is the diffraction angle for the (111) plane. For ceria, the main characteristic peaks are associated with the Face-Centered Cubic (FCC) fluorite structure. The main peak ($2\theta=28.8^\circ$) corresponds to the (111) reflection of ceria and average calculated crystalline size was 17 nm. The main peak ($2\theta=35$ and 38°) corresponds to the CuO and average calculated crystalline size was 19 nm for 7% CuO/CeO₂ and 7% CuO/Ce_{0.9}Mn_{0.1}O₂.

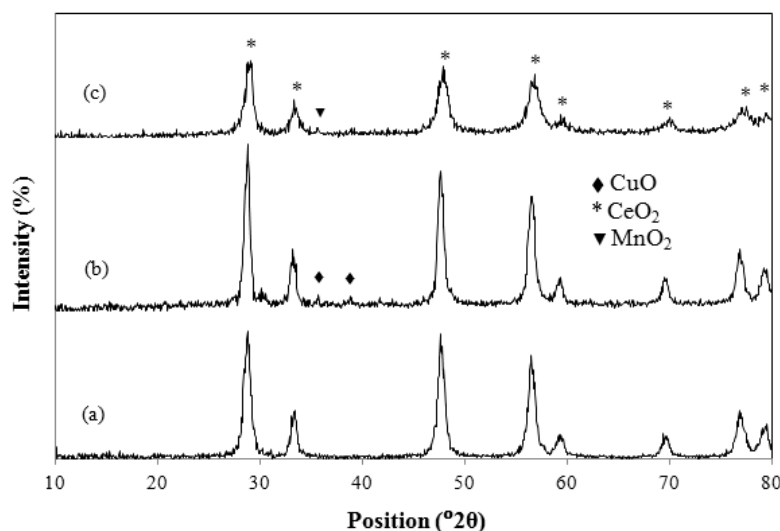


Figure 1. XRD patterns of the samples, (a) CeO₂, (b) 7% CuO/CeO₂ and (c) 7% CuO/Ce_{0.9}Mn_{0.1}O₂.

The TPR patterns for 7% CuO/CeO₂ and 7% CuO/Ce_{0.9}Mn_{0.1}O₂ catalysts are presented in Fig. 2. The 7% CuO/CeO₂ profile shows three peaks between temperatures of 150-250°C, suggesting that the first two peaks correspond to the reduction of CuO species while the third peak is ascribed to the reduction of the surface lattice oxygen in CeO₂ support.

As reported in the previous literature, CuO species identified in CuO/CeO₂ catalysts have been summarized in four types: (1) isolated Cu²⁺ ions can strongly interact with the support. (2) Weak magnetic associates consist of several Cu²⁺ ions and these Cu²⁺ ions have close contact with each other. (3) Small two- and three-dimensional clusters have structures so loose that they have no specific and regular lattice arrangement. (4) Large three-dimensional clusters and bulk CuO phase have characters and properties identical to those of pure CuO powder. Accordingly, it is reasonable to ascribe first peak in the H₂-TPR profiles to the first two types (1 and 2) of CuO species, which is highly dispersed and strongly interacted with the support. The third peak is

ascribed to type (3) CuO species, the small clusters with somehow amorphous properties[4,24-27]. The peak, shown at 500-600°C and 800-900°C, is related to reduction of ceria. In 7% CuO/CeMnO₂ pattern, it can be seen that the density of third peak is lower than 7% CuO/CeO₂, irrespective of peak due to presence of Mn and decline of ceria amount.

3-2. Catalyst activity

3-2-1. Cu and Mn loading effects

The results of Cu loading variation on CO conversion and CO₂ selectivity toward reaction temperature for x% CuO/CeO₂ (x=5, 7 and 10 wt%) catalysts are presented in Fig. 3. As can be seen in Fig. 3, 7% CuO/CeO₂ catalyst has maximum CO conversion in a wide range, and also CO₂ selectivity of this catalyst in lower temperature (<100°C) is more than other catalysts. Therefore, it is obvious that CO oxidation reaction on 7% CuO/CeO₂ is the dominant reaction. In the case of copper catalysts supported on ceria, a partial amount of Cu particles has interaction with CeO₂ and the remaining is in bulk formation.

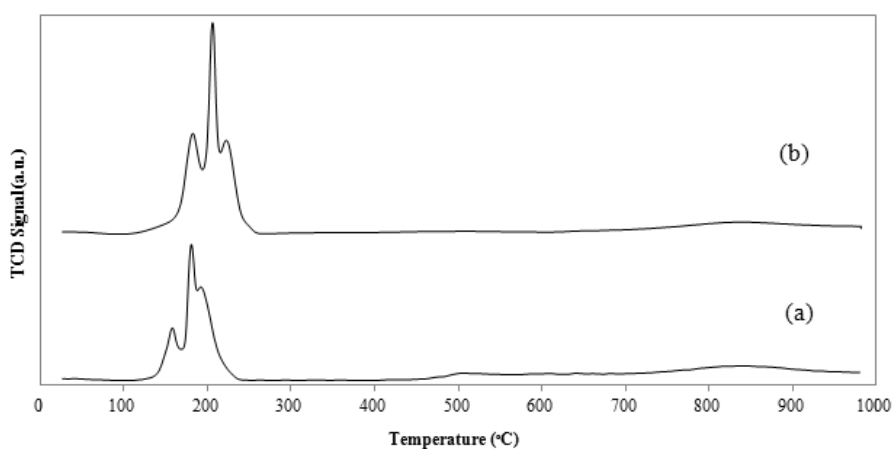


Figure 2. TPR patterns of (a) 7% CuO/CeO₂ and (b) 7% CuO/Ce_{0.9}Mn_{0.1}O₂ catalysts.

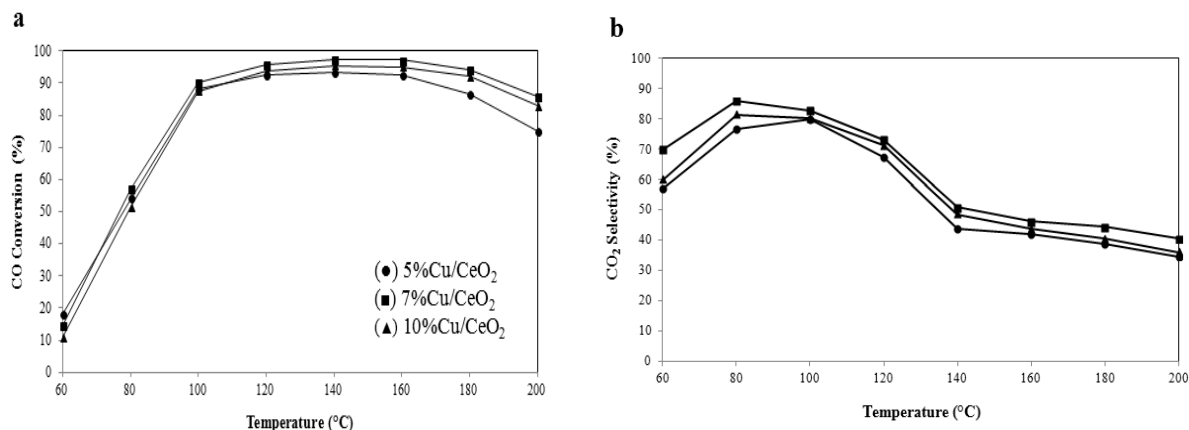


Figure 3. Effect of Cu loading on (a) CO conversion and (b) CO₂ selectivity as a function of temperature. Operating conditions: 96% H₂, 2% CO, 2% O₂, $\lambda=2$, GHSV=20000 h⁻¹.

Gamarra *et al.* reported the CO oxidation on copper oxide species takes place at the interface, while the H₂ oxidation occurs mainly on copper oxide species in the form of nanoparticles, which are not necessarily in contact with the support [28]. Furthermore, an increase in the proportion of CuO species in the bulk form may limit the oxidation of CO because of the decreased number of interfacial sites, while the H₂ oxidation continues to happen on the rest of the supported particles of copper oxide. Thus, the copper species that interact strongly with the support (Cu-O-Ce) are favorable for preferential oxidation of CO [29-31].

Therefore, Cu loading of catalyst for CO-PrOx process has an optimum value to reach more CO conversion with minimum H₂ consumption. Our result showed that 7wt% of Cu is the best content for CuO/CeO₂ catalyst in preferential oxidation process.

The effect of Mn loading as support promoter on activity of 7% CuO supported catalysts is shown in Fig. 4. For Ce_(1-x)Mn_xO₂, (x=0.1, 0.3 and 0.5) composite, the existence of both Ce⁴⁺-Ce³⁺ and Mn⁴⁺-Mn³⁺ redox couples cause excellent oxygen

storage-release capacity, varying with the Ce/Mn ratio [15,32]. It has been seen that increases of Mn content up to 0.1, decreases CO conversion. Mn species enter ceria lattice and increase the mobility of lattice oxygen which leads to their oxygen reacting, but the advantage of manganese oxide is not as much as ceria, so the amount of Mn should not be so much that the effect of ceria decreases and prevents the contact of copper and ceria. For this reason and due to the catalytic activity diagrams, the best amount of Mn is 0.1.

3-2-2. λ Ratio and GHSV effects

The effect of the O₂/CO molar ratio in the feed was analyzed in terms of the oxygen stoichiometric excess (λ). In this work, catalysts were tested in $\lambda \geq 1$. The values of λ lower than 1.0 was not used because the goal of reaching a complete conversion of CO is not possible under such conditions [20]. Fig. 5 shows the CO conversion and CO₂ selectivity as a function of reaction temperature for different λ in the feed composition. As it can be seen in Fig. 5, by increasing λ ratio, the CO conversion increases, but the CO₂ selectivity decreases

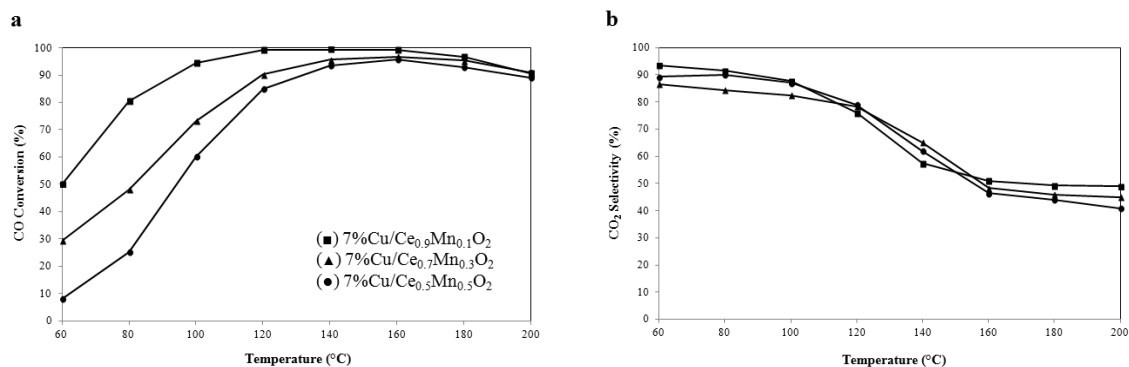


Figure 4. Variation of (a) CO conversion and (b) CO₂ selectivity for 7% CuO/Ce_(1-x)Mn_xO₂ catalysts with different Mn loading. Operating conditions: 96% H₂, 2% CO, 2% O₂, $\lambda=2$, GHSV=20000 h⁻¹.

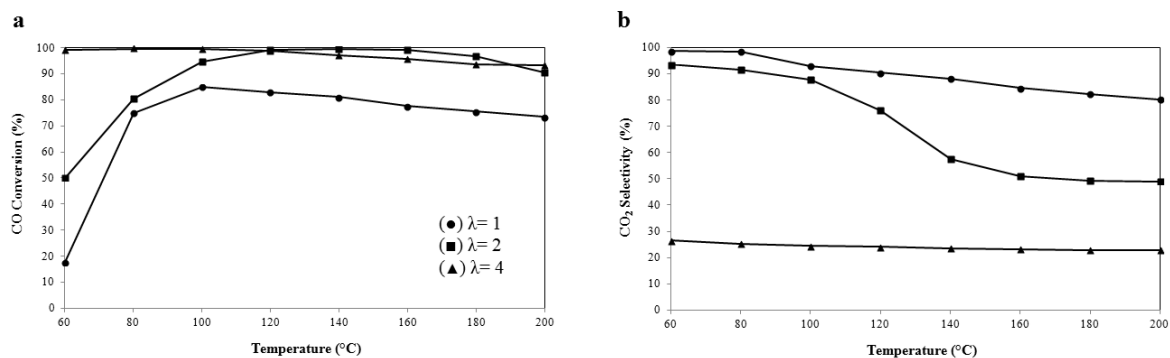


Figure 5. CO-PrOx performance of 7% Cu/Ce_{0.9}Mn_{0.1}O₂ catalyst in different λ . Operating conditions: 96% H₂, 2% CO, 2% O₂, GHSV=20000 h⁻¹.

as in higher λ ratio, more oxygen is accessible to CO and H₂; therefore CO conversion increases and parallel to this the consumption of H₂ increases. Therefore, λ ratio should be optimized. In this work, among the range of λ ($1 \leq \lambda \leq 4$), the results indicate that $\lambda=2$ causes complete conversion of CO in temperature range of 120-200 °C and acceptable CO₂ selectivity in CO-PrOx was observed.

GHSV means quantity of feed processing in a specific time over a constant amount of catalyst, so more GHSV values would cause less used catalyst under constant feed processing, which would result in less reactor

volume, and finally a more economic process would be obtained. As shown in Fig. 6, the higher GHSV has less time over the catalyst to achieve adsorption, thus leading to a lower CO conversion and higher CO₂ selectivity at a specific temperature. At a GHSV of 30000 h⁻¹ and 70% CO conversion, the CO₂ selectivity is around ~100% which is 10% higher than GHSV of 20000 h⁻¹ and 15% higher than GHSV of 10000 h⁻¹.

It is obvious that at temperature below 120°C and at higher GHSV, H₂ adsorption rate was lower than that of CO, thus the CO₂ selectivity was higher. At low GHSV and low temperature, the apparent activation of

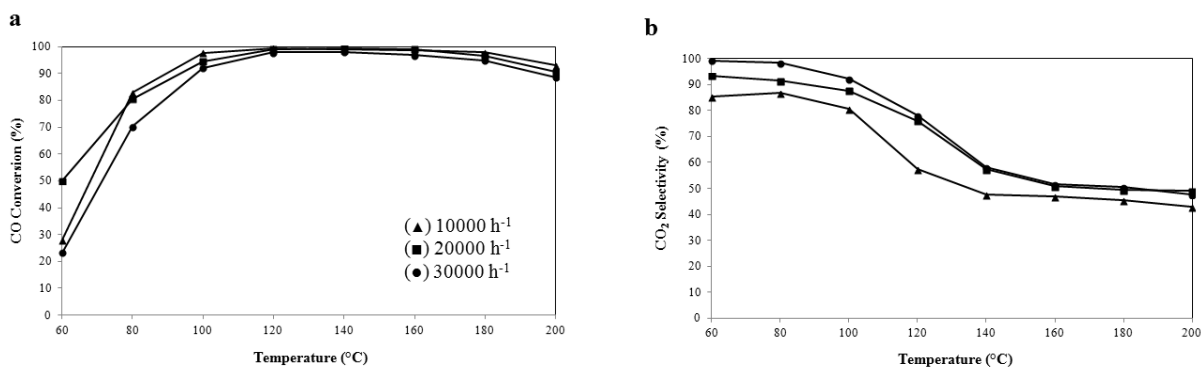


Figure 6. CO-PrOx performance of 7% Cu/Ce_{0.9}Mn_{0.1}O₂ catalyst in different GHSV. Operating conditions: 96% H₂, 2% CO, 2% O₂, $\lambda=2$.

H₂ oxidation is lower than that of CO oxidation [33].

Totally, GHSV should not be so high to decrease the CO conversion, and so low to decrease the CO₂ selectivity. Our results indicated that GHSV of 20000h⁻¹ was appropriate for this catalyst in CO-PrOx.

3-3-3. Effect of H₂O

Since the hydrogen rich stream has been produced by WGS, the reaction contains 10-15% H₂O. The influence of H₂O on the CO-PrOx reaction was investigated. The variation of CO conversion and CO₂ selectivity with the reaction temperature over

7%CuO/Ce_{0.9}Mn_{0.1}O₂ catalyst in the presence of 15% H₂O in feed composition are shown in Fig. 7. It is obvious that the addition of H₂O is not favorable for CO-PrOx. When 15% H₂O is present in the stream, the complete removal of CO cannot be achieved at tested temperature range, while in the absence of H₂O, ~100% CO conversion is obtained at 120°C with 80% CO₂ selectivity. Totally, the negative effect of H₂O on the catalytic performance is related to the blockage of the adsorbed molecular water on the active sites [13]. As a result, the water must be removed before PrOx reactor.

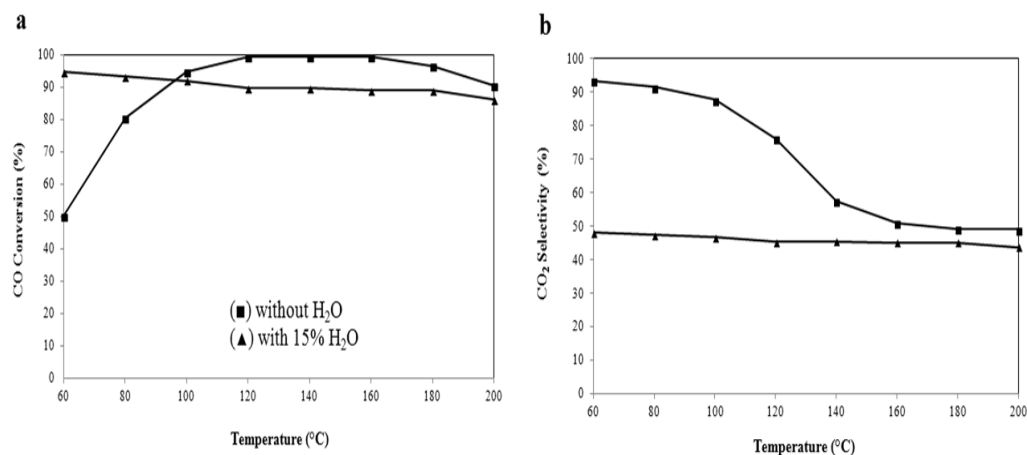


Figure 7. Effect of H₂O on the (a) CO conversion and (b) CO₂ selectivity of 7% Cu/Ce_{0.9}Mn_{0.1}O₂ catalyst. Operating conditions: $\lambda=2$, GHSV=20000 h⁻¹.

3-4. Catalyst stability

The long-term stability of the 7% CuO/Ce_{0.9}Mn_{0.1}O₂ catalyst was evaluated at 120°C during 50 h. Results of CO, O₂ conversion and CO₂ selectivity are reported in Fig. 8. As shown, during all time of stream and nearly hard condition for reaction,

~100% CO conversion was maintained with 70-80% CO₂ selectivity under a GHSV of 20000 h⁻¹ and λ=2. Consequently, it was observed that the 7% CuO/Ce_{0.9}Mn_{0.1}O₂ catalyst has high activity and stability in CO-PrOx conditions.

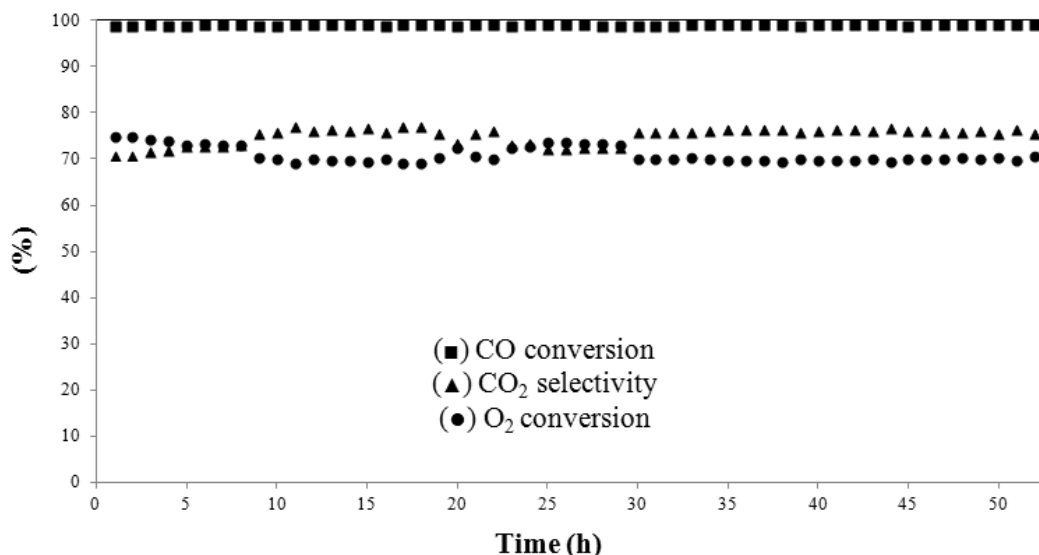


Figure 8. Long-term stability test for CO-PrOx on 7% CuO/Ce_{0.9}Mn_{0.1}O₂ catalyst. Operating conditions: 96% H₂, 2% CO, 2% O₂, λ=2, GHSV=20000 h⁻¹.

4. Conclusions

The performance for CO-PrOx on the CuO/CeO₂ catalysts prepared by wetness impregnation method was investigated. The effects of Cu and Mn loading, λ, GHSV and presence of H₂O in feed on the catalytic activity were evaluated. Results indicate that the catalyst with 7% Cu loading and 0.1 Mn loading has been the best performance among the investigated samples. The 7% CuO/Ce_{0.9}Mn_{0.1}O₂ catalyst has high activity and stability for CO-PrOx and in wide range of reaction temperature (120-160°C) nearly 100% conversion of CO with appropriate CO₂ selectivity was achieved. The presence of H₂O has negative effect on catalyst

activity and the best performance was achieved in λ=2 and GHSV=20000 h⁻¹. In the long-term stability test, ~100% CO conversion with 70-80% CO₂ selectivity was maintained for 50 h at 120°C.

Acknowledgements

This work was supported by Iran Renewable Energy Organization (SUNA).

References

- [1] Alijani, A. and Irankhah, A., "Effect of Nickel Addition on Ceria-Supported Platinum Catalysts for Medium Temperature Shift Reaction in Fuel Processors", *Chem. Eng. Technol.*, **36** (4), 552 (2013).
- [2] Irankhah, A. Rahimi, M. and Rezaei, M., "Performance Research on a Methane Compact Reformer Integrated with Catalytic Combustion", *Chem. Eng. Technol.*, **37** (7), 1220 (2014).
- [3] Kugai, J. Moriya, T. and Seino, S., " γ -Fe₂O₃-supported Pt-Cu nanoparticles synthesized by radiolytic process for catalytic CO preferential oxidation", *J. Appl. Catal. A: General*, **406**, 43 (2011).
- [4] Wu, Z. Zhu, H. and Qin, Z., "CO preferential oxidation in H₂-rich stream over a CuO/CeO₂ catalyst with high H₂O and CO₂ tolerance", *Fuel*, **104**, 41 (2013).
- [5] Mishra, A. and Prasad, R., "A Review on Preferential Oxidation of Carbon Monoxide in Hydrogen Rich Gases", *Bull. Chem. React. Eng. & Catal.*, **6**, 1 (2011).
- [6] Ayastuy, S. J. L. Gonzalez-Marcos, M. P. and Gutierrez, M. A., "Promotion effect of Sn in alumina-supported Pt catalysts for CO-PROX", *Catalysis Communications*, **12**, 895, (2011).
- [7] Bideberripe, H. P. Ramallo-Lopez, J. M. and Figuero, S. J. A., "Ge-modified Pt/SiO₂ catalysts used in preferential CO oxidation (CO-PROX)", *Catalysis Communications*, **12**, 1280 (2011).
- [8] Yang, H. Wang, C. and Li, B., "Doping effects of Ni-MgO on the structure and performance of carbon nanotube-supported Pt catalysts for preferential oxidation of CO in a H₂ stream", *J. Appl. Catal. A: General*, **402**, 168 (2011).
- [9] Desmond, J. W. Zhong, Z. and Luo, "Enhancing preferential oxidation of CO in H₂ on Au/Fe₂O₃ catalyst via combination with APTES/SBA-15 CO₂-sorbent", *J. Hyd. Energy*, **35**, 12724 (2010).
- [10] Meng, M., Tu, Y. and Ding, T., "Effect of synthesis pH and Au loading on the CO preferential oxidation performance of Au/MnO_x-CeO₂ catalysts prepared with ultrasonic assistance", *J. Hyd. Energy*, **36**, 9139 (2011).
- [11] Laguna, O. H. Romero, F. Sarria, M. A. and Centeno, J. A. Odriozola, "Gold supported on metal-doped ceria catalysts (M=Zr, Zn and Fe) for the preferential oxidation of CO (PROX)", *Catal.* **276**, 360 (2010).
- [12] Zhang, Q. and Liu, X., "Manganese-promoted cobalt oxide as efficient and stable non-noble metal catalyst for preferential oxidation of CO in H₂ stream", *J. Appl. Catal. B: Environ.*, **102**, 207, (2011).
- [13] Chen, Y. Z. Liaw, B. J. Wang, J. M. and Huang, C. T. "Selective removal of CO from hydrogen-rich stream over CuO/Ce_xSn_{1-x}O₂-Al₂O₃ catalysts", *Int. J. Hydrogen Energy*, **33**, 2389 (2008).
- [14] Araujo, V. D. Bellido, J. D. A. and Bernardi, M. I. B., "CuO-CeO₂ catalysts synthesized in one-step: Characterization and PROX performance", *J. Hyd. Energy*, **37**, 5498 (2012).
- [15] Zhao, Z. Jin, R. and Bao, T., "Mesoporous Ce_xMn_{1-x}O₂ composites as novel alternative carriers of supported Co₃O₄

- catalysts for CO preferential oxidation in H₂ stream", *J. Hyd. Energy*, **37**, 4774 (2012).
- [16] Varghese, S. Cutrufello, M. G. and Rombi, E., "CO oxidation and preferential oxidation of CO in the presence of hydrogen over SBA-15-templated CuO-Co₃O₄ catalysts", *Appl. Catal. A: Gen.* **443**, 161 (2012).
- [17] Yoshida, Y. Mitani, Y. and Itoi, T., "Preferential oxidation of carbon monoxide in hydrogen using zinc oxide photocatalysts promoted and tuned by adsorbed copper ions", *Catal.*, **287**, 190 (2012).
- [18] Li, X. Quek, X. Y. and Lighthart, M., "CO-PROX reactions on copper cerium oxide catalysts prepared by melt infiltration", *Appl. Catal. B, Environ.*, **424**, 123 (2012).
- [19] Fonseca, J. Ferreira, H. and Bion, N., "Cooperative effect between copper and gold on ceria for CO-PROX reaction", *Catal. Today*, **180**, 34 (2012).
- [20] Marino, F. Schonbrod, B. and Moreno, M., "CO preferential oxidation over CuO-CeO₂ catalysts synthesized by the urea thermal decomposition method", *Catal. Today*, **133**, 735 (2008).
- [21] Moretti, E. Lenarda, M. and Storaro, L., "Preferential CO oxidation (CO-PROX) over CuO-ZnO/TiO₂ catalysts", *J. Appl. Catal. A: General*, **344**, 165 (2008).
- [22] Pakharukova, V. P. Moroz, M. and Kriventsov, V., "Copper-cerium oxide catalysts supported on monoclinic zirconia: Structural features and catalytic behavior in preferential oxidation of carbon monoxide in hydrogen excess", *Appl. Catal. A: Gen.* **365**, 159 (2009).
- [23] Peng, C. T. Lia, H. K. and Liaw, B. J. "Removal of CO in excess hydrogen over CuO/Ce_{1-x}Mn_xO₂ catalysts", *Chem. Eng.* **172**, 452 (2011).
- [24] Zhigang L. Renxian Z. and Xiaoming Z., "Preferential oxidation of CO in excess hydrogen over a nanostructured CuO-CeO₂ catalyst with high surface areas", *Catal. Commun.* **9**, 2183 (2008).
- [25] Xiaolan T. Baocai Zh., Yong L. Yide X. Qin X. and Wenjie S., "CuO/CeO₂ catalysts: Redox features and catalytic behaviors", *Appl. Catal. A: Gen.* **288**, 116 (2005).
- [26] Jong-Won, P. Jin-Hyeok, J. Wang-Lai, Y. Heon, J. Ho-Tae, L. Deuk-Ki, L. Yong-Ki, P. and Young-Woo, R., "Activity and characterization of the Co-promoted CuO-CeO₂/γ-Al₂O₃ catalyst for the selective oxidation of CO in excess", *Appl. Catal. A: Gen.* **274**, 25 (2004).
- [27] Aboukais, A. Bennani, A. and Lamonier-Dulongpont, C., "Redox behaviour of copper(II) species on CuCe oxide catalysts: electron paramagnetic resonance (EPR)", *Colloid. Surf. A.*, **115**, 171 (1996).
- [28] Gamarra, D. Belver, C. and Fernandez-Garcia, M., "Selective CO Oxidation in Excess H₂ over Copper-Ceria Catalysts: Identification of Active Entities/Species", *Am. Chem. Soc.*, **129**, 12064 (2007).
- [29] Avgouropoulos, G. Ioannides, T. and Matralis, H., "Influence of the preparation method on the performance of CuO-CeO₂ catalysts for the selective oxidation of CO", *Appl. Catal. B: Environ.*, **56**, 87 (2005).
- [30] Polster, C. and Baertsch, C.,

"Application of CuO_x-CeO₂ catalysts as selective sensor substrates for detection of CO in H₂ fuel", *Chem. Commun.*, **35**, 4046 (2008).

[31] Gamarra, D. Munuera, G. and Hungria, A., "Theoretical Study of Catalytic CO Oxidation on (111) Metal Surfaces: Calculating Rate Constants That Account for Tunnel Effect", *Phys. Chem.*, **111**, 11026 (2007).

[32] Azalim, S. Franco, M. Brahmi, R. Giraudon, J., "Removal of oxygenated volatile organic compounds by catalytic oxidation over Zr-Ce-Mn catalysts", *J. Hazard. Mater.*, **188**, 422. (2011).

[33] Cominos, V. Hessel, V. and Hofmann, C., "Selective oxidation of carbon monoxide in a hydrogen-rich fuel cell feed using a catalyst coated microstructured reactor", *Catal. Today*, **110**, 140 (2005).

[34] Estifae, P. Haghghi, M. Mohammadi, N. and Rahmani, F., "CO oxidation over sonochemically synthesized Pd-Cu/Al₂O₃ nanocatalyst used in hydrogen purification: Effect of Pd loading and ultrasound irradiation time", *Ultrasonics Sonochem.*, **21** (3), 1155 (2014).

[35] Fattah, Z. Rezaei, M. Biabani-Ravandi, A. and Irankhah, A., "Preparation of Co-MgO mixed oxide nanocatalysts for low temperature CO oxidation: Optimization of preparation conditions", *Proc. Saf. Environ. Protec.*, **92** (6), 948 (2014).